JOC The Journal of Organic Chemistry

Article

pubs.acs.org/joc

Detection of Amines with Extended Distyrylbenzenes by Strip Assays

Jan Kumpf,[†] Jan Freudenberg,[†] Katharyn Fletcher,[‡] Andreas Dreuw,[‡,§] and Uwe H. F. Bunz*[,†,§]

[†]Organisch-Chemisches Institut, Ruprecht-Karls-Universität Heidelberg, Im Neuenheimer Feld 270, 69120 Heidelberg, Germany

[‡]Interdisziplinäres Zentrum für Wissenschaftliches Rechnen, Ruprecht-Karls Universität Heidelberg, Im Neuenheimer Feld 368, 69120 Heidelberg, Germany

[§]Centre of Advanced Materials, Ruprecht-Karls-Universität Heidelberg, Im Neuenheimer Feld 225, 69120 Heidelberg, Germany

Supporting Information

ABSTRACT: We herein describe the synthesis and property evaluation of three novel aldehyde-substituted pentameric phenylenevinylenes carrying branched oligo(ethylene glycol) (swallowtail, Sw) substituents. The targets were synthesized by a combination of Heck coupling and Wittig or Horner reactions of suitable precursor modules. If the pentameric phenylenevinylene carries only two of these Sw substituents, it is no longer water-soluble. When six of the Sw substituents are attached, regardless of their position, the pentameric phenylenevinylenes are well water-soluble. The dialdehydes were investigated with respect to their amine-sensing capabilities both in water as well as in the solid state, sprayed onto thin layer chromatography (TLC) plates (alox, silica gel, reversed phase silica gel). The recognition of amine vapors using the sprayed-on phenylenevinylene dialdehydes is superb and allows the identification of different amines on regular silica TLC plates via color changes, analyzed by a statistical tool, the multivariate analysis of variance (MANOVA) protocol.

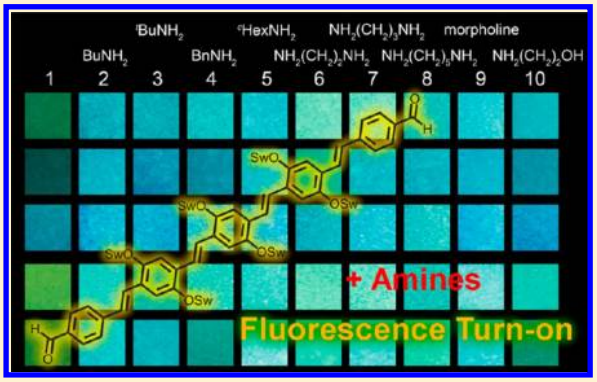

INTRODUCTION

The sensing and detection of amines is an important and attractive scientific and practical proposition. Amines are almost ubiquitous analytes that play significant roles in areas ranging from food freshness determination (spoilage of fresh fish, meat, and shellfish),[1] disease state evaluation (amine content in breath of patients with bronchial or lung diseases including cancer) but are also part of industrial effluvia, as amines are used in the production of fertilizers, pharmaceuticals, surfactants, and colorants.[2] Cell sensing applications to gain insight into distribution and/or presence of biogenic amines and neurotransmitters are also attractive.[3] A wide variety of different approaches has been employed to sense amines, including but not restricted to proton transfer protocols,[4] aggregation and change of conformation of macromolecules,[5] as well as the color change of solvatochromic porphyrine-based dyes.[6] An alternative approach uses chemodosimeters, in which the amine under consideration reacts with the fluorophore or chromophore and changes its structure, its electronic makeup, and consequently the absorption and emission spectra. Particularly interesting are carbonyl groups; a series of highly electrophilic trifluoromethylarylketones[7] was deployed as substrates to react with amines. Also, tricyanovinyl groups[8] react with protic analytes under addition and therefore change of their electronic etc. properties.

Our approach exploits simple aryl aldehydes to detect primary and secondary amines.[9] Either distyrylbenzenes or cruciform fluorophores that are organo- or water-soluble were employed. In the case of the water-soluble, swallowtail (Sw) substituted distyrylbenzenes such as **1**, primary amines are quickly detected in water at relatively low concentrations. The simple distyrylbenzene derivatives just as well as the somewhat more complex cruciform fluorophores are, if aldehyde substituted, capable of detecting amines by either imine[10] or aminal formation. Here we investigate the synthesis and properties of larger, pentameric phenylene-vinylene based dialdehydes and explore their amine dosimetric properties in aqueous solution and as thin-sprayed films on solid supports. We investigated the effect of the size of the π-system but also the number and position of the Sw substituents on the π-conjugated backbone. We find that both number and position of the Sw substituents have an influence on the amine reactivity of the oligophenylenevinylenes.

RESULTS AND DISCUSSION

Synthesis. We have identified Sw substituents as superb in both to add water solubility to conjugated materials but also to significantly increase the fluorescence quantum yields of conjugated polymers and small molecules.[11] The Sw substituents render the aromatic backbones soluble in water but

Received: May 22, 2014

   dx.doi.org/10.1021/jo501129d | J. Org. Chem. XXXX, XXX, XXX−XXX

Scheme 1. Synthesis of 4

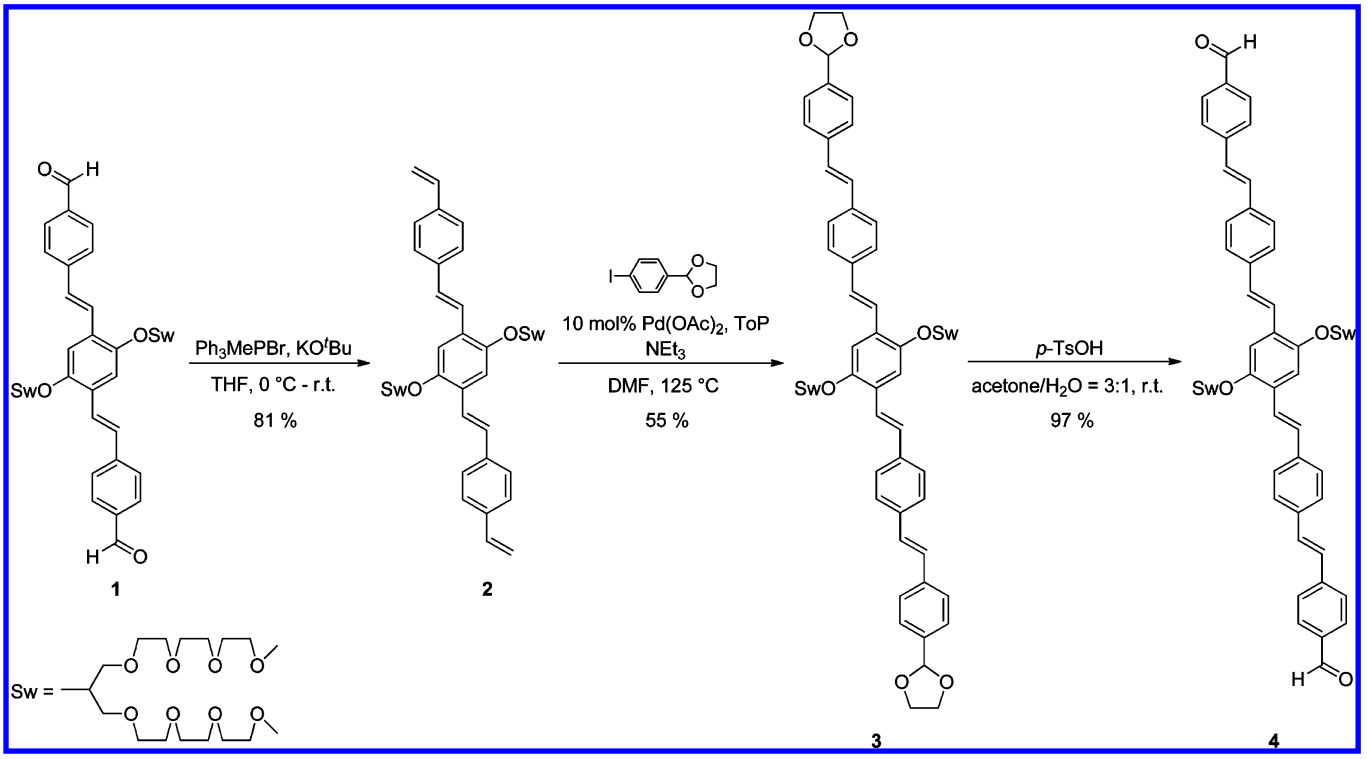

Scheme 2. Synthesis of Buildings Blocks 9 and 11

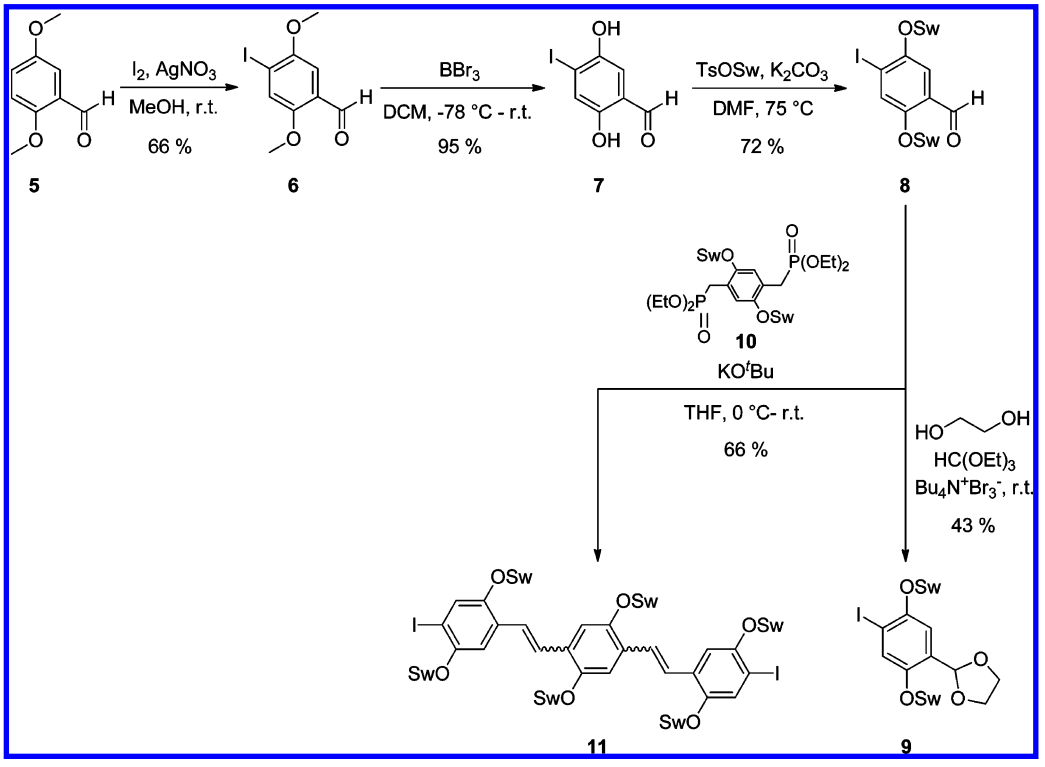

also in organic solvents such as dichloromethane or chloroform. Only hexane is a poor solvent for Sw-equipped arenes.

We first prepared compound **4**, which carries two supporting Sw substituents (Scheme 1). Starting from distyrylbenzene **1**, a Wittig reaction furnishes the moderately stable divinyl compound **2**, which is Heck-coupled to the ethylene glycol acetal of 4-iodobenzaldehyde into the extended pentameric phenylenevinylene **3**. *p*-TsOH then leads to smooth, quantitative deprotection, and **4** is isolated. Compound **4** is not very well soluble in water but can be dissolved in a 9:1 mixture of water and THF.

The synthesis of **4** is straightforward. For the preparation of **13** and **16**, slightly more complex synthetic approaches are employed. Starting from **5** (Scheme 2), electrophilic iodination

dx.doi.org/10.1021/jo501129d | J. Org. Chem. XXXX, XXX, XXX−XXX

Scheme 3. Synthesis of Compound 13

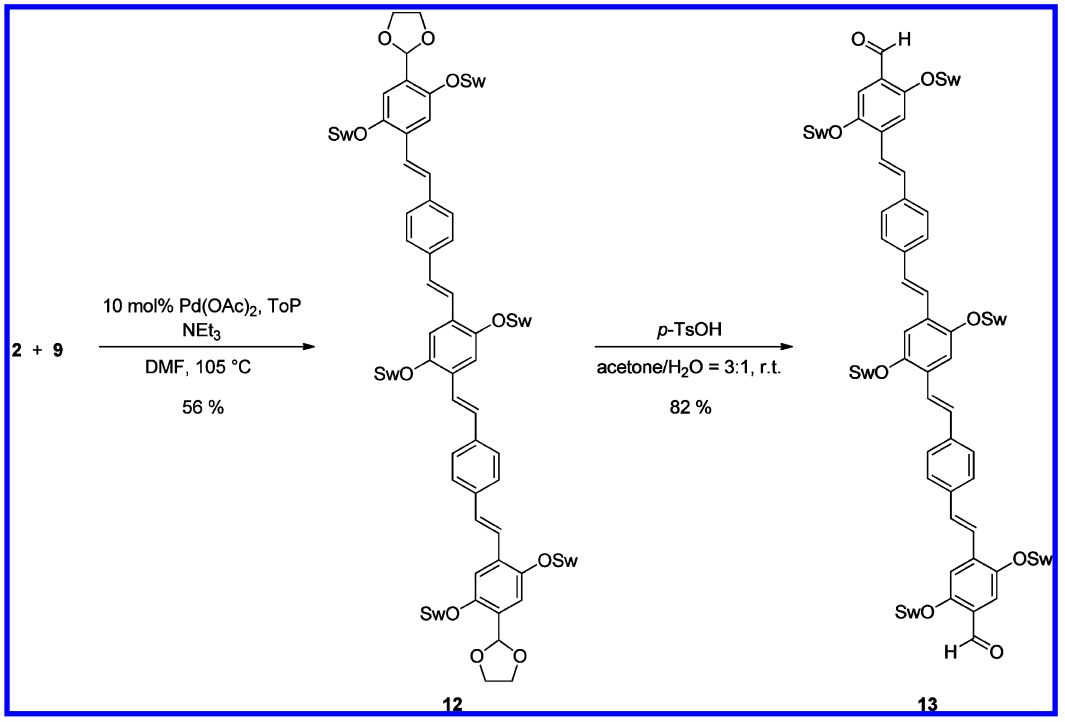

Scheme 4. Synthesis of Compound 16

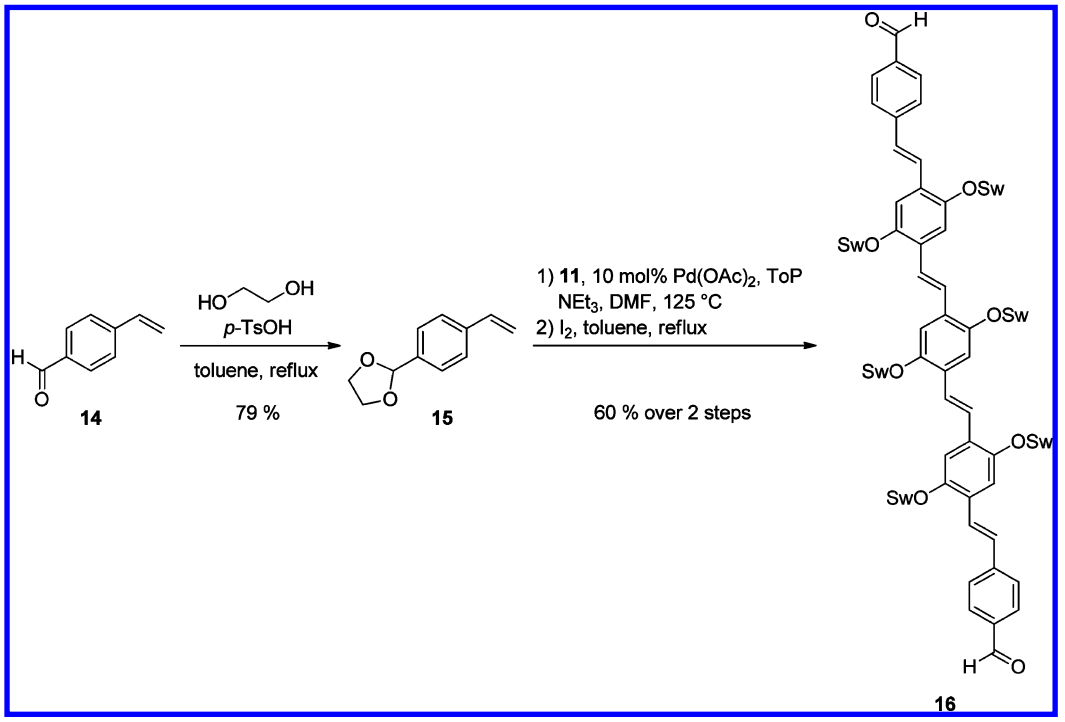

furnishes **6**. This selectivity is unusual, as the aldehyde group is apparently not *meta*- but *para*-directing, similar to examples found by MacLachlan.[12] BBr_3 demethylates **6**, and coupling to the Sw tosylate at elevated temperatures gave the iodobenzaldehyde **8** in good yield. Acetalization furnishes **9**, and subsequent reaction of **8** with the bisphosphonate **10** gives **11** as an inseparable mixture of *E*- and *Z*-isomers. We possess all modules to construct the pentamers **13** and **16**. Combining **2** and **9** in the presence of $Pd(OAc)_2$ and tri(*o*-tolyl)phosphine (ToP) (Scheme 3) forms **12**, which upon reaction with *p*-TsOH gives the target molecule **13** in 82% yield.

To obtain the isomer **16** (Scheme 4), 4-vinylbenzaldehyde is protected to give the acetal **15**, which was Heck-coupled with **11**. A mixture of *cis*- and *trans*-isomers formed, which was equilibrated into the all-*trans*-isomer and deprotected by a catalytic amount of iodine at reflux temperature, thus forming **16** in 60% yield starting from **15**.

Optical Properties. We looked at the optical properties and the amine-sensing usefulness of **4**, **13**, and **16**. Figure 1

dx.doi.org/10.1021/jo501129d | J. Org. Chem. XXXX, XXX, XXX−XXX

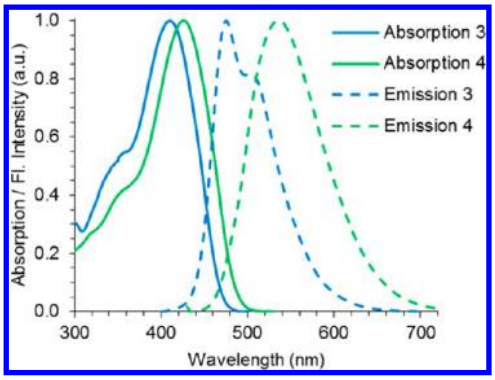

Figure 1. Absorption and emission spectra of **3** and **4** in dichloromethane.

shows the UV−vis and emission spectra of **3** and **4** both in dichloromethane and in water, while in Figure 2 the absorption and emission spectra of **12**, **13**, and **16** in dichloromethane and in water are shown. The compounds **3** and **4** carrying only two Sw units each are not water-soluble but still dissolve well in DCM or THF. Table 1 compares the photophysical properties of all of the compounds. In DCM all of the investigated phenylenevinylenes display fluorescence quantum yields ranging from 75% to 80%. Also, the emission data are all similar, regardless if acetals or the aldehydes were investigated. Only for the pair **3** and **4** $\lambda_{max,em}$ is red-shifted upon deprotection.

Compounds **3** and **4** are insoluble in water, but for **12**, **13**, and **16** quantum yields and emission maxima in water can be gleaned (Table 1). Surprisingly, the $\lambda_{max,em}$ values for **12**, **13**, and **16** in water are very similar, i.e., the addition of the aldehyde groups, which leads to a larger π-system, is not reflected in a red-shift of their emission spectra. However, for the absorption spectra a red-shift is observed when going from **12** to **13**.

The presence of the aldehyde groups has a significant effect on the emission quantum yield ϕ_f of **12**, which drops from 0.22 to <0.005 upon deprotection into **13**. Fluorescence quenching is due to an excitation-induced protonation/deprotonation mechanism of the aldehyde group in protic solvents, as has been previously shown for smaller distyrylbenzene dialdehydes.[9c] This mechanism nicely explains why aromatic aldehydes generally possess lower fluorescence quantum yields in water than in aprotic solvents.

Excited State Properties. Quantum chemical calculations at the theoretical level of time-dependent density functional theory (TDDFT)[13] in combination with the standard B3LYP functional and the 6-31G* basis set have been performed to gain insight into the influence of substitution of the pentameric phenylenevinylene core. For these calculations, first the ground state geometries were optimized (DFT/B3LYP/6-31G*) for the molecules **3m**, **4m**, **12m**, **13m**, and **16m**, in which the Sw substituents were replaced by OMe groups for computational efficiency. In addition, the vertical excitation energies have been computed in the gas phase, as well as with a polarizable continuum model for water as implemented in Orca 2.9.[14] For the computation of the vertical excitation energies of the optically allowed $\pi\pi$*-excited state of these compounds, this approach is sufficiently accurate.[15]

According to our TDDFT results, the S_1 state of all investigated pentameric phenylenevinylene model compounds **3m**, **4m**, **12m**, **13m**, and **16m** is a strongly allowed $\pi\pi$* excited state with a huge oscillator strength that dominates the experimental absorption spectra and the optical properties of these compounds. In the molecular orbital picture, the S_1 state corresponds to the promotion of an electron from the HOMO to the LUMO (Figure 3), and these frontier MOs of all investigated molecules are practically identical and indistinguishable. HOMO and LUMO are concentrated on the central rings, and hence, substitution of these rings with OSw tails will have a different influence on the excitation energy of the S_1 state. Substitution on the central ring will lead to a larger red-shift of the absorption than substitution on the outer rings. This is the case, as the calculated excitation energies of **13m** and **16m** and measured absorption wavelengths of **13** and **16** reveal

Table 1. Photophysical Properties of 3, 4, 12, 13, and 16 Recorded in DCM and in Water

compd	$\lambda_{max,abs}$ (nm)	$\lambda_{max,em}$ (nm)	Stokes shift (cm^{-1})	$\Phi_f \pm 5$ (%)	τ_f (ns)	ε ($dm^3/(mol\cdot cm)$)
			In DCM			
3	410	475	3337	76	1.2	57284
4	426	536	4817	75	1.6	63478
12	426	527	4499	80	1.2	69933
13	435	542	4538	77	1.6	80963
16	443	544	4191	77	1.5	70921
			In Water			
12	412	480, 510	4664	22	1.3	66184
13	434	474, 508	1944	<0.5	1.3	74468
16	437	517	3541	<0.5	1.1	67525

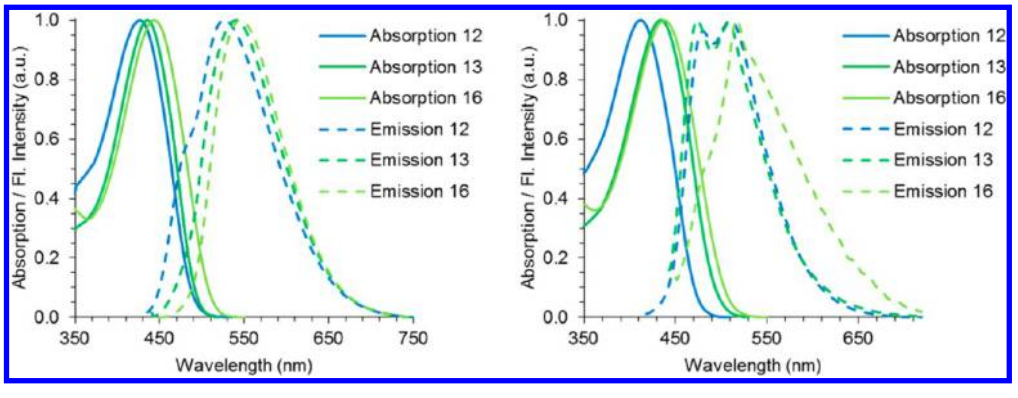

Figure 2. Absorption and emission spectra of **12**, **13**, and **16** in dichloromethane (left) and in water (right).

dx.doi.org/10.1021/jo501129d | J. Org. Chem. XXXX, XXX, XXX−XXX

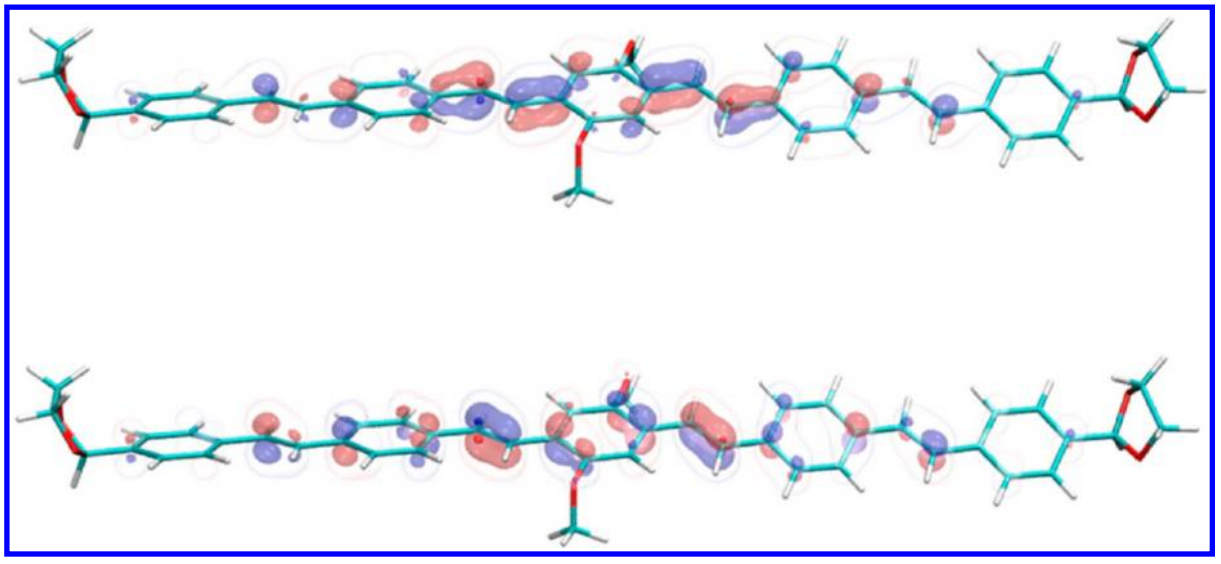

Figure 3. Highest occupied (HOMO, bottom) and lowest unoccupied molecular orbital (LUMO, top) of model compound **3m**. The orbitals of the other model compounds are practically indistinguishable.

(Table 2 and Table 1). The calculations explain why deprotection of the aldehydes has a smaller influence on the absorption wavelength, because the involved orbitals are practically not influenced by the substitution. A small red-shift is still observed because the LUMO of the aldehydes is slightly more extended than the LUMO of the acetals.

Table 2. Computed Vertical Excitation Energies of the S_1 states of 3m, 4m, 12m, 13m, and 16m at the theoretical level of TDDFT/B3LYP/6-31G*

compd	excitation energy (eV)	λ_{max} (nm)	oscillator strength
	In Vacuum		
3m	2.57	482	3.41
4m	2.45	506	3.27
12m	2.55	486	3.46
13m	2.40	517	3.36
16m	2.28	543	2.86
	In Water		
3m	2.35	528	3.23
4m	2.28	543	3.26
12m	2.49	498	3.56
13m	2.32	534	3.46
16m	1.99	623	3.13

Amine Dosimetry. Aldehyde functionalities react with primary and secondary amines under formation of aminals (1,*n*-diamines), imines (primary amines), and hemiaminals (secondary amines). The adduct formation leads in all cases to changes in the absorption and or emission spectra. In a first experiment, we investigated solutions of **4** in water/THF = 9:1 (c = 4.4 μM) (Figure 4) with the amines 2−11.

In the water/THF solvent mix, some of the amines show responses toward **4**. Addition of butylamine or benzylamine leads to orange emission, while 1,3-diaminopropane gives a change of the emission to intensely turqueois. Figure 5 shows the respective emission spectra. One sees the large turn-on upon addition of 1,3-diaminopropane, which significantly differs from the reaction of **4** with either ethylenediamine or with cadaverine. Ethanolamine and 4-aminopyridine also lead to a somewhat blue-shifted absorption and emission features.

The aldehydes **13** and **16** react much more predictable toward the addition of amines in water. The aqueous solutions of the dialdehydes are practically nonfluorescent. Addition of amines leads mostly to a fluorescence turn-on with some shift of the emission wavelength (Figure 6). Both **13** and **16** react similarly, and their reactivity is most pronounced at pH 11. While there is still some amine reactivity at pH 9, at pH 7 the aldehydes are almost unchanged, when the amines are added. At pH 7 the amines are fully protonated and therefore do not react with the aldehydes to the imines.

Figure 4. Photographs of solutions of **4** in water/THF = 9:1 (c = 4.4 μM) upon addition of amines 2−12 (left to right): (1) fluorophore reference, (2) butylamine, (3) *tert*-butylamine, (4) benzylamine, (5) cyclohexylamine, (6) ethylenediamine, (7) 1,3-diaminopropane, (8) cadaverine, (9) morpholine, (10) ephedrine, (11) 4-aminopyridine, (12) ethanolamine. The samples were illuminated using a hand-held UV lamp at an emission wavelength of 365 nm. Photographs were taken with fixed settings of the camera (JPEG format, shutter speed 0.05 s, ISO value 100, aperture F2.8, white balance 6500 K, and Adobe RGB 1986 color space).

dx.doi.org/10.1021/jo501129d | *J. Org. Chem.* XXXX, XXX, XXX−XXX

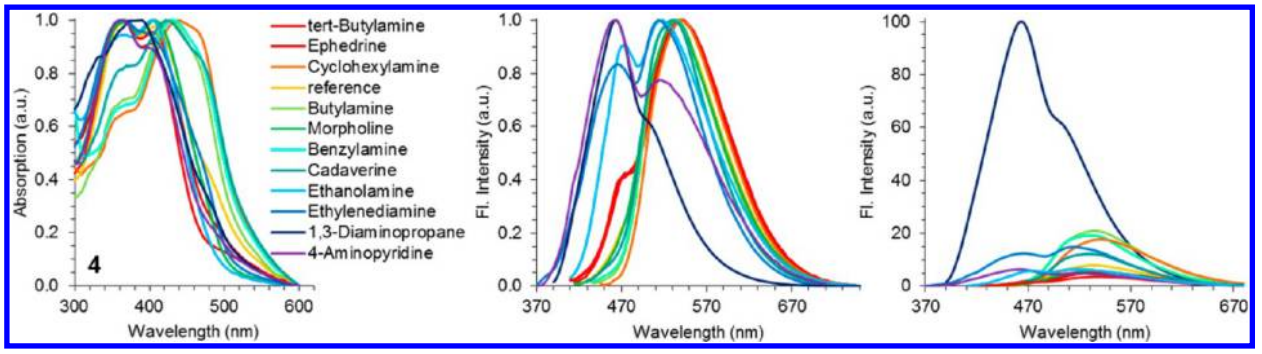

Figure 5. Absorption spectra (left), emission spectra (middle), and non-normalized emission spectra (right) of solutions of **4** in water/THF = 9:1 upon addition of different amines.

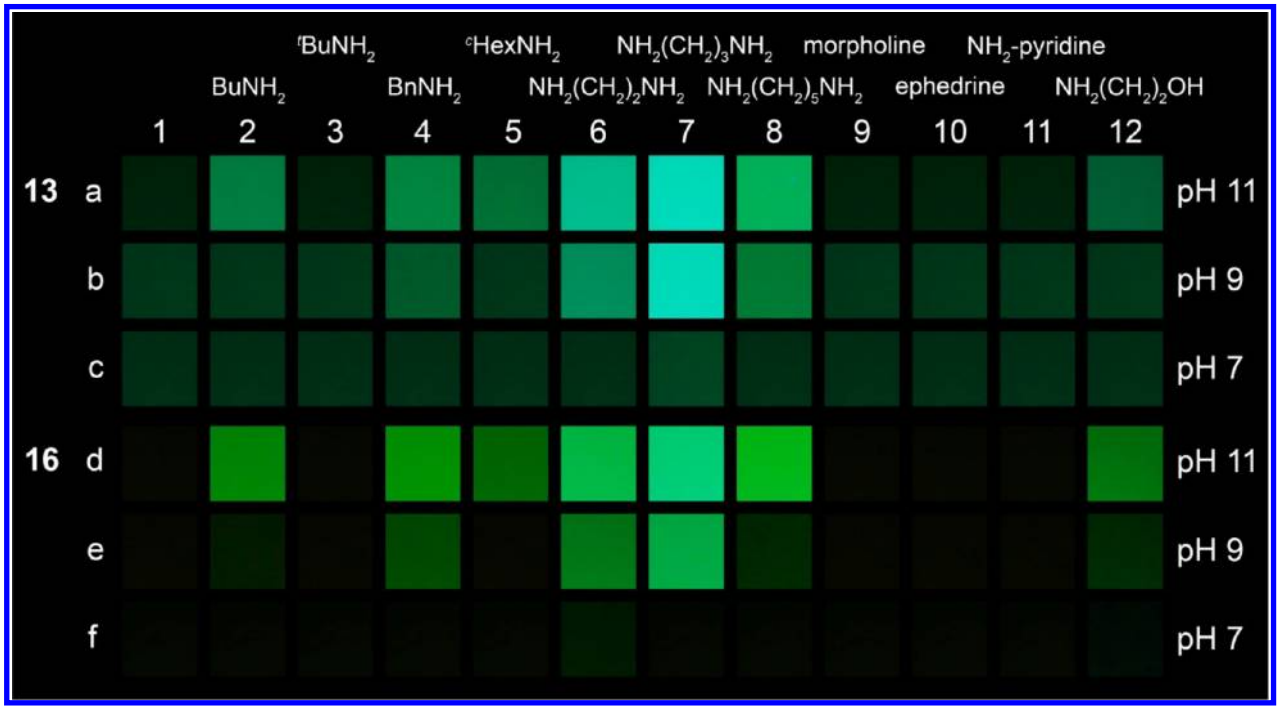

Figure 6. Photographs of buffered aqueous solutions (c = 4.4 μM) of **13** (a–c) and **16** (d–f) upon addition of amines 2–12 (left to right). Buffers: pH 11 (a, d), pH 9 (b, e), pH 7 (c, f). Columns: (1) fluorophore reference, (2) butylamine (10.43), (3) *tert*-butylamine (10.45), (4) benzylamine (9.34), (5) cyclohexylamine (10.64), (6) ethylenediamine (6.90/9.95), (7) 1,3-diaminopropane (8.49/10.47), (8) cadaverine (9.58/10.85), (9) morpholine (8.36), (10) ephedrine (10.14), (11) 4-aminopyridine (9.12), (12) ethanolamine (9.50). The samples were excited using a hand-held UV lamp at an emission wavelength of 365 nm. Photographs were taken with fixed settings of the camera (JPEG format, shutter speed 0.05 s, ISO value 100, aperture F2.8, white balance 6500 K, and Adobe RGB 1986 color space). The numbers in paratheses give the pK_a of the ammonium salts.

In Figure 7 the corresponding absorption and emission spectra are shown (at pH 9 and pH 11). Whereas for **13** the optical data only change subtly upon addition of most amines, cadaverine gives a red-shifted emission profile. In all of the other cases the shifts are less pronounced. However, if one looks at the intensity information, one can see that the fluoresecene turn-on is cadaverine < 1,2-ethylenediamine < 1,3-diaminopropane.

In the case of **16**, the spectral shifts upon addition of amines at pH 11 or pH 9 are even less distinct than for **13** or **4**, but the turn-on upon the addition of 1,3-diaminopropane is distinct. The other amines show only a slight increase in emission intensity upon imine formation. Figure 8 depicts the time-dependent increase of the fluorescence intensity upon addition of 1,3-diaminopropane to **13** or **16**. For **13** the fluorescence turn-on is practically finished after 10 min and the fluorescence intensity has increased approximately 60 times. The isomer **16** reaches the same turn-on factor after 6–7 min but continues to increase in intensity, until a turn-on factor of >140 is achieved after 20 min. While **13** is more reactive and reaches saturation in half the time, **16** shows a significantly increased turn-on. It is tempting to attribute the faster reaction of **13** with the amines toward a hydrogen-bonded precomplex that should not be possible in **16**, therefore leading to lower reaction rates.

Figure 9 explores the sensitivity of the reactions of **13** and **16** with 1,3-diaminopropane. Compound **13** seems to be a bit more sensitive than **16**, as the fluorescence turn-on is already quite distinct at 5.5 ppm; in both cases the response is almost complete at a concentration of 55 ppm (0.75 mM) of 1,3-diaminopropane.

Loosely speaking, the amine reactivities of **13** and **16** are similar and are also similar to that of the smaller distyrylbenzene derivative **1**, investigated earlier. While sensing of amines in water is important, it is also attractive to see if

dx.doi.org/10.1021/jo501129d | *J. Org. Chem.* XXXX, XXX, XXX–XXX

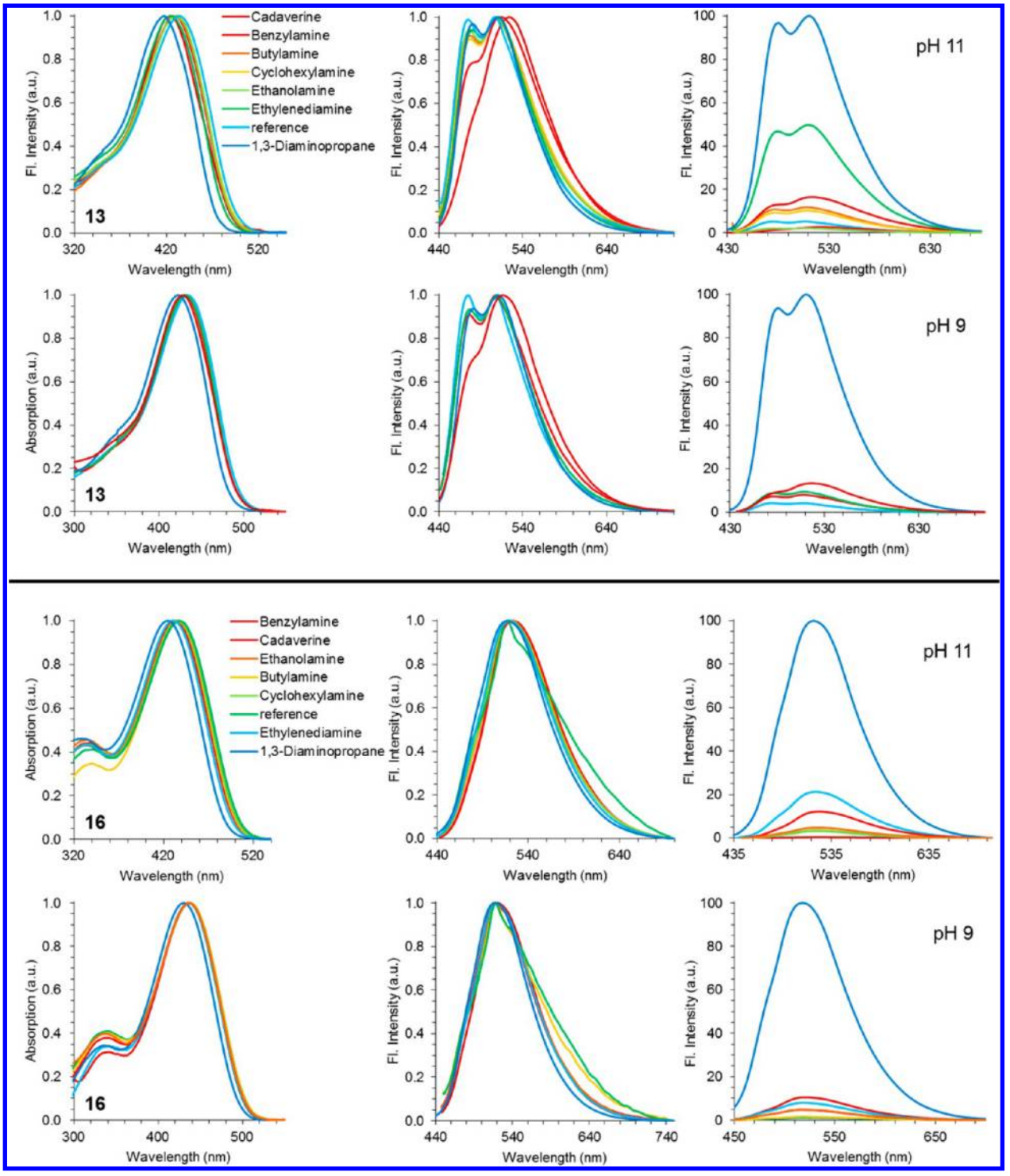

Figure 7. Absorption spectra (left), normalized emission spectra (middle), and non-normalized emission spectra (right) of buffered aqueous solutions (top: pH 11, bottom: pH 9) of **13** and **16** upon addition of different amines.

amine vapors could be detected by our aldehydes. Toward that end, we constructed test strips, in which we sprayed the fluorogenic aldehydes **1**, **4**, **13**, **16**, and **17** (structure in Figure 10) onto solid supports, here silica gel, reverse phase silica gel, and also neutral alox thin layer chromatography (TLC) plates. The dissolved fluorophores were sprayed onto the solid supports using a perfume atomizer. Then the plates were cut into strips, and each strip was exposed to a specific amine vapor in addition to a reference strip. Figure 11 shows the fluorescence responses. To evaluate these plots, we used the brightness-independent color coordinates rg of the RAW data of the photographs of the exposed strips.[16] These rg values were determined for every square in the panel (Figure 11) and were treated with multivariate analysis of variance (MANOVA) statistics:[17]

$$\sigma_{m,n}(\mathrm{r},\,\mathrm{g}) = \sqrt{\frac{\sum_{\mathrm{dye5}}^{\mathrm{dye1}} (\mathrm{r}_n - r_m)^2 + (\mathrm{g}_n - \mathrm{g}_m)^2}{3 \times 5}}$$

dx.doi.org/10.1021/jo501129d | J. Org. Chem. XXXX, XXX, XXX−XXX

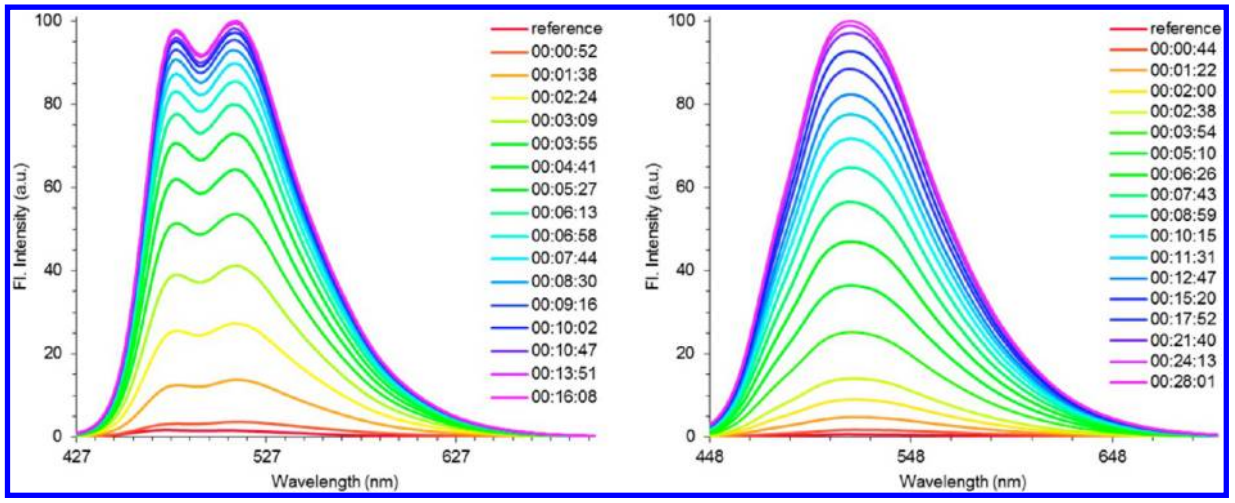

Figure 8. Time-dependent evolution of the emission wavelength and emission intensity for the reactions of **13** (left) and **16** (right) in a buffered aqueous solution (pH 11, c = 0.9 μM) with 1,3-diaminopropane (120 ppm (vol)).

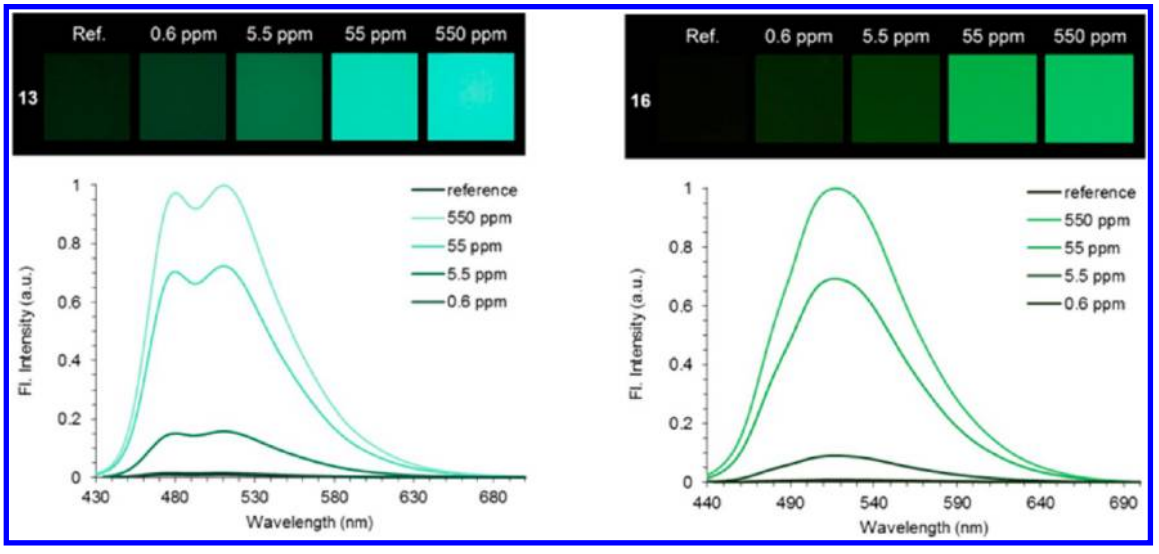

Figure 9. Photographs and fluorescence spectra of buffered aqueous solutions (pH 11, c = 4.4 μM) of **13** (left) and **16** (right) at the concentrations of 1,3-diaminopropane specified in the panel.

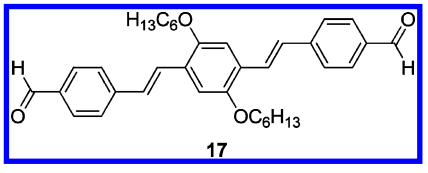

Figure 10. Structure of compound **17**.

In this correlation the photographic data were classified into a neutral alox, silica gel, or reversed phase silica gel based sensor array. The autocorrelation plot for each sensor array (silica, reversed phase silica, alox) is shown in Figure 12. All of the diagonal squares are and must be black (i.e., the color difference between the two compared patches are zero), as their color is identical by definition. In an ideal case, all of the other patches would have large color differences as expressed by the MANOVA calculation and lighter color. The lighter the off-diagonal values are, the better the differentiation of the two amines under consideration. As the matrices are symmetrical, one would only need the upper or the lower diagonal part of the matrix. The discrimination is particularly good when the dyes are cast onto regular silica gel, and only butylamine and *tert*-butylamine are difficult to distinguish, while benzylamine, structurally similar, gives a different response. All of the other amines are easily discerned. Consequently, these strips made from five structurally similar dialdehydes (two distyrylbenzenes and three pentameric species) are powerful in identifying and discerning amine vapors when photographs taken under blacklight are evaluated by statistical analysis of the color information.

■ CONCLUSION

We have prepared water-soluble pentameric phenylenevinylene dialdehydes and investigated their amine sensing capabilities both in water as well as using solid strips for amine vapors. The solid-state sensing approach is powerful and simple. The strip sensors discerned a series of primary and secondary amines by applying a MANOVA statistics evaluation to photographs of the vapor-exposed strips. The strips contain five different phenylenevinylene dialdehydes that differentiate all of the investigated amines. In future we will prepare further aldehyde and functionally appended phenylenevinylenes as potent amine

dx.doi.org/10.1021/jo501129d | J. Org. Chem. XXXX, XXX, XXX−XXX

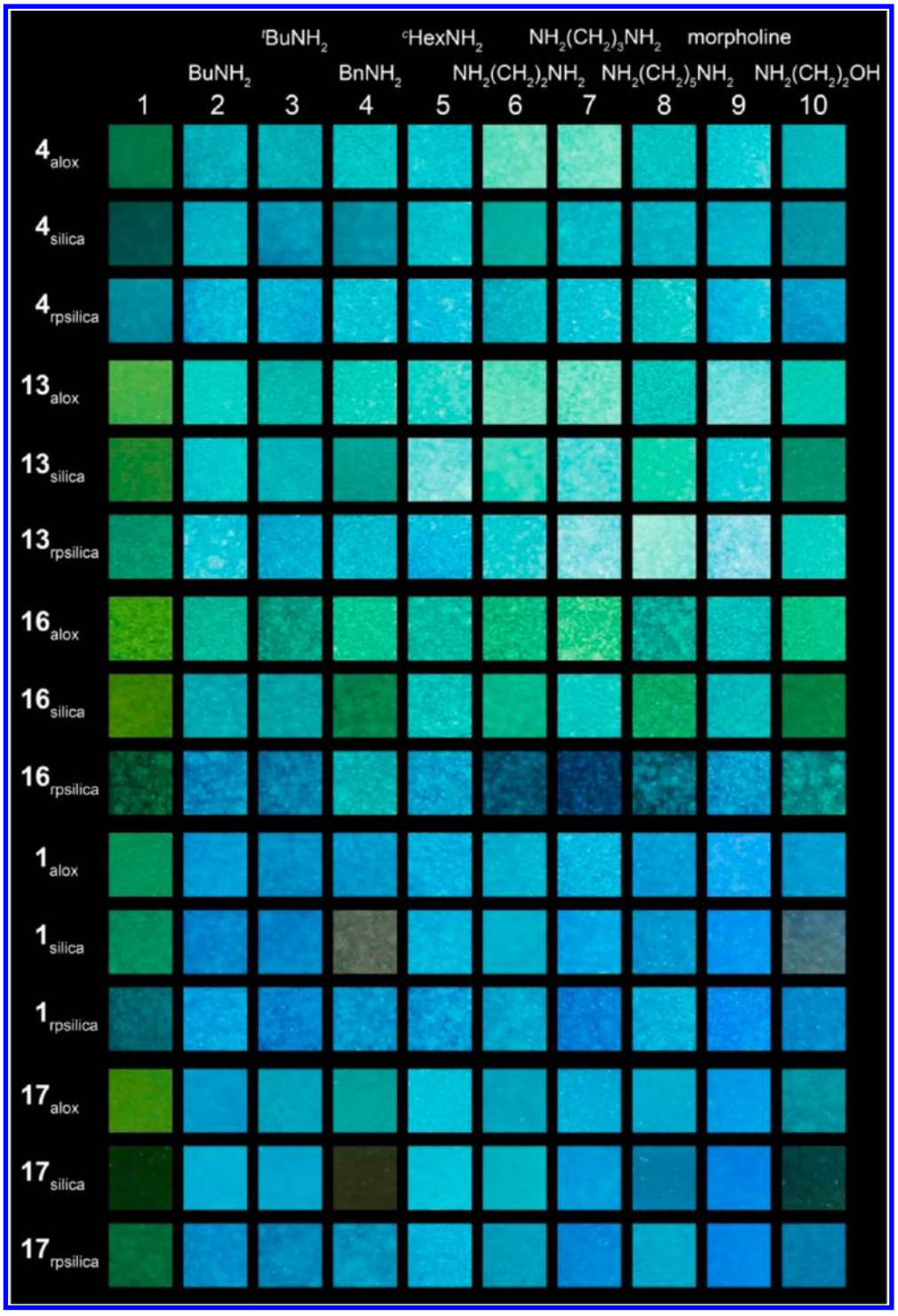

Figure 11. Photographs of samples of **4**, **13**, **16**, **1**, and **17** on alox, silica gel, and reversed phase silica gel TLC plates after 20 h of exposure to amine vapors 2−10 (left to right). Columns: (1) fluorophore reference, (2) butylamine, (3) *tert*-butylamine, (4) benzylamine, (5) cyclohexylamine, (6) ethylenediamine, (7) 1,3-diaminopropane, (8) cadaverine, (9) morpholine, (10) ethanolamine. The samples were illuminated using a hand-held UV lamp at an emission wavelength of 365 nm and photographs were taken with fixed settings of the camera (JPEG format, shutter speed 0.05 s, ISO value 100, aperture F2.8, white balance 6500 K, and Adobe RGB 1986 color space).

sensors. We will look at the structure and support-dependent limit of detection and identification for amine vapors in these easily constructed strip assays. Photographic methods combined with MANOVA statistics are supremely useful for the quick extraction of information pertaining to sensory events under change of emission color.

EXPERIMENTAL SECTION

All reagents and solvents were obtained from commercial suppliers and were used without further purification unless otherwise noted. Preparation of air- and moisture-sensitive materials was carried out in oven-dried flasks under a nitrogen atmosphere using Schlenk techniques. Compounds **1**,[9c] **6**,[18] **7**,[19] **10**,[9d] and **14**[20] were prepared as reported. ^{1}H NMR spectra were recorded on a 300, 400, or 600

dx.doi.org/10.1021/jo501129d | J. Org. Chem. XXXX, XXX, XXX−XXX

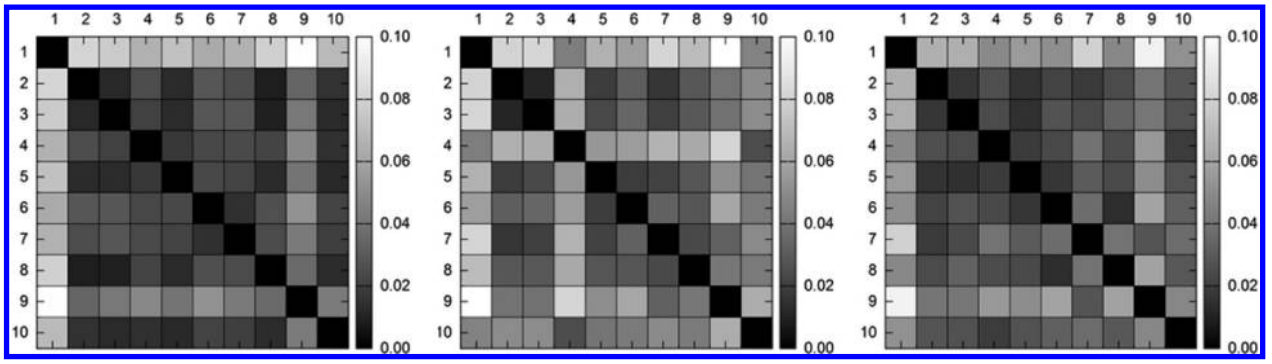

Figure 12. Autocorrelation plot (RAW rg values) of fluorescent dyes **1**, **4**, **13**, **16**, and **17** on neutral alox (left), silica gel (middle), and reversed phase silica gel (right) after exposure to amines recorded with a digital camera. When color information on identical amines + dyes are correlated the deviation $\sigma_{n,m}$ disappears (black squares on the diagonal).

MHz spectrometer, and ^{13}C NMR spectra were recorded on a 75, 100, or 150 MHz spectrometer. Chemical shifts (δ) are reported in parts per million (ppm) relative to traces of $CHCl_3$.[21] MS spectra were recorded using fast atom bombardment, electrospray ionization, direct analysis in real-time or electron impact detected by magnetic sector and FT-ICR techniques, respectively. Infrared (IR) spectra are reported in wavenumbers (cm^{-1}) and were recorded neat. Absorption and emission spectra were recorded in dichloromethane and water/buffered solutions. Quantum yields Φ were obtained by the absolute method using an Ulbricht sphere.[22] Time-correlated single photon counting lifetime measurements were made with a pulsed laser diode.

13,13′-[(2,5-Bis((*E*)-4-vinylstyryl)-1,4-phenylene)bis(oxy)]bis-(2,5,8,11,15,18,21,24-octaoxapentacosane) (2). Methyltriphenylphosphonium bromide (712 mg, 1.99 mmol, 2.20 equiv) was suspended in dry THF (4 mL), and the suspension was cooled to 0 °C. KO^{t}Bu (223 mg, 1.99 mmol, 2.20 equiv) was added, and the mixture was stirred at 0 °C for 1 h before the dialdehyde **1** (1.00 g, 906 μmol, 1.00 equiv) was added carefully. The reaction mixture was stirred at 0 °C for 30 min and then at room temperature overnight. The reaction was quenched by addition of a saturated aqueous solution of NH_4Cl (10 mL). The layers were separated, and the aqueous layer was extracted with dichloromethane (4 × 10 mL). The combined organic layers were dried over $MgSO_4$, and the solvents were evaporated. The crude product was purified by column chromatography (silica gel, petroleum ether/dichloromethane/ethyl acetate/methanol = 5:3:1:0.5, R_f = 0.16) and further by gel permeation chromatography (polystyrene beads 200−400 mesh, toluene) to yield **2** as a bright yellow oil (803 mg, 730 μmol, 81%). IR (cm^{-1}): 2868, 1694, 1598, 1511, 1488, 1455, 1415, 1349, 1295, 1249, 1198, 1096, 969, 848, 827, 727. ^1H NMR (300 MHz, $CDCl_3$): δ 7.52−7.46 (m, 6H), 7.40 (d, J = 8.3 Hz, 4H), 7.33 (s, 2H), 7.06 (d, J = 16.4 Hz, 2H), 6.72 (dd, J = 17.6 Hz, 11.0 Hz, 2H), 5.76 (d, J = 17.6 Hz, 2H), 5.25 (d, J = 11.0 Hz, 2H), 4.51 (quin, J = 5.0 Hz, 2H), 3.79−3.77 (m, 8H), 3.71−3.56 (m, 40H), 3.52−3.48 (m, 8H), 3.34 (s, 12H). ^{13}C NMR (100 MHz, $CDCl_3$): δ 151.1, 137.6, 136.9, 136.6, 128.9, 128.6, 126.9, 126.7, 123.3, 114.3, 113.7, 79.8, 72.0, 71.2, 70.8−70.6 (m, (20C), 59.1. HRMS (ESI): m/z [M + Na]$^+$ calcd for $C_{60}H_{90}O_{18}Na$ 1121.6025, found 1121.6044; m/z [M + K]$^+$ calcd for $C_{60}H_{90}O_{18}K$ 1137.5764, found 1137.5771.

2,2′-(((1*E*,1′*E*)-(((1*E*,1′*E*)-(2,5-Bis(2,5,8,11,15,18,21,24-octaoxapentacosan-13-yloxy)-1,4-phenylene)bis(ethene-2,1-diyl))bis(4,1-phenylene))bis(ethene-2,1-diyl))bis(4,1-phenylene))bis(1,3-dioxolane) (3). The reaction was performed in a heat-gun-dried 25 mL Schlenk tube under a nitrogen atmosphere. Compound **2** (200 mg, 182 μmol, 1.00 equiv) and 2-(4-iodophenyl)-1,3-dioxolane (110 mg, 400 μmol, 2.20 equiv) were dissolved in dry DMF (6 mL). $Pd(OAc)_2$ (4.08 mg, 18.2 μmol, 0.10 equiv), tris(*o*-tolyl)phosphine (22 mg, 72.8 μmol, 0.40 equiv) and triethylamine (0.5 mL) were added. The mixture was stirred at 120 °C for 72 h. After the reaction mixture was cooled to room temperature, it was poured into water (50 mL) to give a yellow suspension that was extracted with dichloromethane (4 × 50 mL) until the aqueous layer was colorless. The combined organic layers were washed with brine and dried over $MgSO_4$. The solvents were removed under reduced pressure. The brown residue was purified by column chromatography (silica gel, petroleum ether/dichloromethane/ethyl acetate/methanol = 5:3:1:0.5, R_f = 0.09), which yielded **3** as a highly viscous dark yellow oil (97.0 mg, 69.5 μmol, 38%). IR (cm^{-1}): 2871, 1611, 1514, 1487, 1454, 1417, 1389, 1349, 1302, 1249, 1197, 1079, 964, 942, 823, 749, 551. ^1H NMR (300 MHz, $CDCl_3$): δ 7.56−7.46 (m,18H), 7.36−7.33 (m, 2H), 7.13(s, 4H), 7.08 (d, J = 16.4 Hz, 2H), 5.83 (s, 2H), 4.53 (quin, J = 5.0 Hz, 2H), 4.18−4.03 (m, 8H), 3.80−3.78 (m, 8H), 3.70−3.57 (m, 40H), 3.51−3.48 (m, 8H), 3.34 (s, 12H). ^{13}C NMR (150 MHz, $CDCl_3$): δ 151.0, 138.4, 137.5, 137.1, 136.5, 129.0, 128.6, 128.6, 128.0, 127.1, 127.0, 127.0, 126.6, 123.3, 114.2, 103.7, 79.8, 72.0, 71.2, 70.8, 70.7−70.6, 65.4, 59.2. HRMS (ESI): m/z [M + Na]$^+$ calcd for $C_{78}H_{106}O_{22}Na$ 1417.7073, found 1417.7068; m/z [M + K]$^+$ calcd for $C_{78}H_{106}O_{22}K$ 1433.6813, found 1433.6807.

4,4′-(((1*E*,1′*E*)-(((1*E*,1′*E*)-(2,5-Bis(2,5,8,11,15,18,21,24-octaoxapentacosan-13-yloxy)-1,4-phenylene)bis(ethene-2,1-diyl))bis(4,1-phenylene))bis(ethene-2,1-diyl))dibenzaldehyde (4). In a 10 mL round bottomed flask dioxolane **3** (74.0 mg, 53.0 μmol, 1.00 equiv) was suspended in 4 mL of a 3:1 mixture of acetone and water. Then a catalytic amount of *p*-toluenesulfonic acid was added, and the suspension was stirred at room temperature overnight. The resulting solution was quenched with a saturated aqueous $NaHCO_3$ solution (10 mL), and dichloromethane (20 mL) was added. The layers were separated, and the aqueous layer was extracted with dichloromethane (4 × 20 mL). The combined organic layers were dried over $MgSO_4$, and the solvents were evaporated. Column chromatography (silica gel, petroleum ether/dichloromethane/ethyl acetate/methanol = 5:3:1:0.6, R_f = 0.17) afforded **4** as a highly viscous yellow oil (67.0 mg, 51.2 μmol, 97%). IR (cm^{-1}): 2865, 1687, 1593, 1566, 1514, 1479, 1451, 1415, 1349, 1328, 1304, 1250, 1209, 1197, 1163, 1139, 1100, 969, 945, 906, 864, 845, 826, 791, 756, 546. ^1H NMR (300 MHz, $CDCl_3$): δ 10.00 (s, 2H), 7.88 (d, J = 8.2 Hz, 4H), 7.67 (d, J = 8.2 Hz, 4H), 7.58−7.52 (m, 10H), 7.36 (s, 2H), 7.28 (d, J = 16.2 Hz, 2H), 7.16 (d, J = 16.5 Hz, 2H), 7.09 (d, J = 16.5 Hz, 2H), 4.54 (quin, J = 4.8 Hz, 2H), 3.81−3.79 (m, 8H), 3.71−3.57 (m, 40H), 3.51−3.48 (m, 8H), 3.34 (s, 12H). ^{13}C NMR (75 MHz, $CDCl_3$): δ 191.7, 151.2, 143.6, 138.3, 135.9, 135.4, 132.0, 130.4, 129.0, 128.5, 127.4, 127.2, 127.0, 123.9, 114.3, 79.8, 72.0, 71.2, 70.9, 70.7−70.6, 59.1. HRMS (ESI): m/z [M + H]$^+$ calcd for $C_{74}H_{99}O_{20}$ 1307.6730, found 1307.6775.

2,5-Bis(2,5,8,11,15,18,21,24-octaoxapentacosan-13-yloxy)-4-iodobenzaldehyde (8). In a 25 mL Schlenk flask K_2CO_3 (314 mg, 2.27 mmol, 6.00 equiv) was added to a solution of swallowtail tosylate (449 mg, 833 μmol, 2.20 equiv) in DMF (5 mL). The suspension was degassed. Then aldehyde **7** (100 mg, 379 μmol, 1.00 equiv) was added, and the mixture was stirred at 75 °C for 48 h. The reaction mixture was poured into water (40 mL) to give an off-white suspension that was extracted with dichloromethane (6 × 50 mL). The combined organic extracts were washed with brine and dried over $MgSO_4$. The crude product was purified by column chromatography (silica gel, petroleum ether/dichloromethane/ethyl acetate/methanol = 5:3:1:0.6,

dx.doi.org/10.1021/jo501129d | J. Org. Chem. XXXX, XXX, XXX−XXX

R_f = 0.14) to afford **8** as a yellow oil (275 mg, 276 μmol, 73%). IR (cm^{-1}): 2919, 2857, 1682, 1588, 1463, 1390, 1350, 1298, 1253, 1200, 1097, 937, 849, 742. ^1H NMR (300 MHz, $CDCl_3$): δ 10.37 (s, 1H), 7.69 (s, 1H), 7.37 (s, 1H), 4.51 (quin, *J* = 5.0 Hz, 2H), 3.76−3.71 (m, 8H), 3.67−3.60 (m, 40H), 3.55−3.52 (m, 8H), 3.37 (s, 12H). ^{13}C NMR (150 MHz, $CDCl_3$): δ 189.5, 155.9, 152.7, 128.5, 127.0, 111.8, 97.8, 80.3, 79.9, 72.0, 71.3, 71.2, 70.8−70.6, 59.2. HRMS (ESI): *m*/*z* $[M + Na]^+$ calcd for $C_{41}H_{73}IO_{19}Na$ 1019.3688, found 1019.3687; *m*/*z* $[M + K]^+$ calcd for $C_{41}H_{73}IO_{19}K$ 1035.3428, found 1035.3416.

2-(2,5-Bis(2,5,8,11,15,18,21,24-octaoxapentacosan-13-yloxy)-4-iodophenyl)-1,3-dioxolane (9). To a solution of **8** (300 mg, 1.30 mmol, 1.00 equiv) and triethyl orthoformate (153 μL, 1.43 mmol, 1.10 equiv) in ethylene glycol (1 mL) was added tetrabutylammonium tribromide (5.55 mg, 13.0 μmol, 0.01 equiv). The reaction mixture was stirred at room temperature for 72 h. The reaction mixture was purified directly by column chromatography (silica gel, petroleum ether/dichloromethane/ethyl acetate/methanol = 5:3:1:0.6, R_f = 0.12) to yield **9** as a yellow oil (152 mg, 555 μmol, 43%). IR (cm^{-1}): 2870, 1473, 1391, 1350, 1292, 1251, 1198, 1098, 941, 849, 761. ^1H NMR (400 MHz, $CDCl_3$): δ 7.51 (s, 1H), 7.14 (s, 1H), 6.04 (s, 1H), 4.45 (quin, *J* = 5.0 Hz, 1H), 4.38 (quin, *J* = 5.0 Hz, 1H), 4.11−3.95 (m, 4H), 3.75−3.62 (m,48H), 3.54−3.52 (m, 8H), 3.37 (s, 12H). ^{13}C NMR (100 MHz, $CDCl_3$): δ 152.5, 152.0, 129.3, 127.3, 113.7, 98.9, 89.2, 80.1, 80.0, 72.1, 71.3, 71.2, 70.8−70.7, 65.3, 59.2. HRMS (ESI): *m*/*z* $[M + Na]^+$ calcd for $C_{43}H_{77}IO_{20}Na$ 1063.3951, found 1063.3949; *m*/*z* $[M + K]^+$ calcd for $C_{43}H_{77}IO_{20}K$ 1079.3690, found 1079.3683.

13-[2,5-Bis{(*E*)-2-[4-iodo-2,5-bis(2,5,8,11,15,18,21,24-octaoxapentacosan-13-yloxy)phenyl]ethenyl}-4-(2,5,8,11,15,18,21,24-octaoxapentacosan-13-yloxy)phenoxy]-2,5,8,11,15,18,21,24-octaoxapentacosane (11). Bisphosphonate **10** (200 mg, 175 μmol, 1.00 equiv) was dissolved in dry THF (5 mL). The solution was cooled to 0 °C, and KO^{t}Bu (45.0 mg, 402 μmol, 2.30 equiv) was added. The mixture was stirred at 0 °C for 10 min before aldehyde **8** (366 mg, 175 mmol, 2.10 equiv) was added. The reaction mixture was allowed to reach room temperature and stirred for 3 d. The reaction was quenched by addition of a saturated NH_4Cl solution (20 mL). The layers were separated, and the aqueous layer was extracted with DCM (5 × 20 mL). The combined organic extracts were washed with brine and dried over $MgSO_4$, and the solvents were removed by rotary evaporation. Purification by column chromatography (silica gel, petroleum ether/dichloromethane/ethyl acetate/methanol = 5:3:1:1.5, R_f = 0.33) afforded a mixture of *E*- and *Z*-isomers of **11** (328 mg, 116 μmol, 66%), which was used in the next step without further purification. HRMS (MALDI): *m*/*z* $[M + H]^+$ calcd for $C_{124}H_{221}O_{54}I_2$ 2828.2637, found 2828.2752.

2,2′-{[2,5-Bis(2,5,8,11,15,18,21,24-octaoxapentacosan-13-yloxy)benzene-1,4-diyl]bis{(*E*)ethene-2,1-diylbenzene-4,1-diyl-(*E*)ethene-2,1-diyl[2,5-bis(2,5,8,11,15,18,21,24-octaoxapentacosan-13-yloxy)benzene-4,1-diyl]}}bis(1,3-dioxolane) (12). The reaction was performed in a heat-gun-dried 25 mL Schlenk tube under a nitrogen atmosphere. Compounds **2** (100 mg, 91.0 μmol, 1.00 equiv) and **9** (208 mg, 200 μmol, 2.20 equiv) were dissolved in dry DMF (4 mL). $Pd(OAc)_2$ (2.00 mg, 9.10 μmol, 0.10 equiv), tris(*o*-tolyl)phosphine (11 mg, 36.4 μmol, 0.40 equiv), and triethylamine (0.5 mL) were added. The mixture was stirred at 105 °C for 72 h. After the reaction mixture was cooled to room temperature, it was poured into 50 mL of water to give a brown suspension that was extracted with dichloromethane (5 × 50 mL) until the aqueous layer was colorless. The combined organic layers were washed with brine and dried over $MgSO_4$. The solvents were removed under reduced pressure. The brown residue was purified by column chromatography (silica gel, petroleum ether/dichloromethane/ethyl acetate/methanol = 5:3:1:1.5, R_f = 0.22) to give **12** as a highly viscous yellow oil (149 mg, 50.9 μmol, 56%). IR (cm^{-1}): 2868, 1609, 1489, 1455, 1416, 1350, 1251, 1196, 1099, 962, 849, 734, 530. ^1H NMR (300 MHz, $CDCl_3$): δ 7.52−7.50 (m, 10H), 7.46 (d, *J* = 5.8 Hz, 2H), 7.32 (d, *J* = 2.5 Hz, 4H), 7.21 (s, 2H), 7.10−7.03 (m, 4H), 6.11 (s, 2H), 4.57−4.48 (m, 6H), 4.15−3.96 (m, 8H), 3.80−3.75 (m, 24H), 3.69−3.57 (m, 120H), 3.53−3.48 (m, 24H), 3.35−3.33 (m, 36H). ^{13}C NMR (150 MHz, $CDCl_3$): δ 151.6, 151.0, 150.5, 137.3, 137.1, 130.0, 129.2, 129.1, 128.9, 128.7, 128.6, 128.2, 127.1, 127.0, 123.1, 115.2, 114.0, 113.5, 99.0, 79.5, 79.4, 79.2, 72.0−71.9, 71.2−71.1, 70.8−70.6, 65.3, 59.2−59.1. HRMS (MALDI): *m*/*z* $[M]^+$ calcd for $C_{146}H_{242}O_{58}$ 2923.5987, found 2923.6151.

4,4′-{[2,5-Bis(2,5,8,11,15,18,21,24-octaoxapentacosan-13-yloxy)benzene-1,4-diyl]bis[(*E*)ethene-2,1-diylbenzene-4,1-diyl-(*E*)ethene-2,1-diyl]}bis[2,5-bis(2,5,8,11,15,18,21,24-octaoxapentacosan-13-yloxy)benzaldehyde] (13). Compound **12** (129 mg, 44.1 μmol, 1.00 equiv) was dissolved in acetone/water = 3:1 (12 mL acetone + 4 mL water), and a catalytic amount of *p*-toluenesulfonic acid was added. The solution was stirred at room temperature overnight. The reaction was quenched by addition of a saturated aqueous solution of $NaHCO_3$ (5 mL) and dichloromethane (10 mL). The layers were separated, and the aqueous layer was extracted with dichloromethane (4 × 20 mL). The combined organic extracts were washed with brine and dried over $MgSO_4$, and the solvents were evaporated to yield **13** as a dark yellow oil (102 mg, 40.0 μmol, 82%). IR (cm^{-1}): 2867, 2361, 1675, 1592, 1481, 1418, 1349, 1288, 1251, 1197, 1098, 965, 849, 719. ^1H NMR (300 MHz, $CDCl_3$): δ 10.40 (s, 2H), 7.55−7.47 (m, 14H), 7.42 (s, 2H), 7.35 (s, 2H), 7.19 (d, *J* = 16.4 Hz, 2H), 7.09 (d, *J* = 16.4 Hz, 2H), 4.66 (quin, *J* = 5.0 Hz, 2H), 4.57 (quin, *J* = 4.8 Hz, 4H), 3.80−3.76 (m, 24H), 3.69−3.57 (m, 120H), 3.53−3.48 (m, 24H), 3.36−3.34 (m, 36H). ^{13}C NMR (150 MHz, $CDCl_3$): δ 189.4, 156.1, 151.0, 150.7, 138.0, 136.5, 135.9, 132.0, 128.9, 128.5, 127.5, 127.1, 126.1, 123.5, 122.5, 114.0, 113.8, 79.7, 79.5, 78.9, 72.0, 72.0, 71.2−71.1, 70.8−70.6, 59.2, 59.2. HRMS (MALDI): *m*/*z* $[M + H]^+$ calcd for $C_{142}H_{235}O_{56}$ 2836.5541, found 2836.5610.

2-(4-Vinylphenyl)-1,3-dioxolane (15). The reaction was performed in a 100 mL round-bottomed flask equipped with a Dean−Stark distilling receiver. A solution of 4-ethenylbenzaldehyde (2.60 g, 19.7 mmol, 1.00 equiv), ethylene glycol (8.54 mL, 197 mmol, 10.0 equiv), and a catalytic amount of *p*-toluenesulfonic acid in toluene (60 mL) was refluxed (140 °C) for 6 h. Then the reaction mixture was quenched with a saturated aqueous solution of $NaHCO_3$ (40 mL). The phases were separated, and the aqueous layer was extracted with dichloromethane (3 × 50 mL). The combined organic layers were washed with brine (60 mL) and dried over $MgSO_4$, and the solvents were removed *in vacuo*. Purification of the crude product by column chromatography (silica gel, petroleum ether/ethyl acetate = 15:2, R_f = 0.21) yielded **15** as a colorless oil (2.73 g, 15.5 mmol, 79%). ^1H NMR (300 MHz, $CDCl_3$): δ 7.47−7.41 (m, 4H), 6.73 (dd, *J* = 17.6 Hz, 10.9 Hz, 1H), 5.82 (s, 1H), 5.77 (d, *J* = 17.6 Hz, 1H), 5.26 (d, *J* = 10.9 Hz, 1H), 4.16−4.01 (m, 4H). ^{13}C NMR (75 MHz, $CDCl_3$): δ 138.6, 137.5, 136.6, 126.8, 126.3, 114.6, 103.7, 65.4. HRMS (EI): *m*/*z* $[M]^+$ calcd for $C_{11}H_{12}O_2$ 176.0837, found 176.0838.

4,4′-{[2,5-Bis(2,5,8,11,15,18,21,24-octaoxapentacosan-13-yloxy)benzene-1,4-diyl]bis[(*E*)ethene-2,1-diyl[2,5-bis-(2,5,8,11,15,18,21,24-octaoxapentacosan-13-yloxy)benzene-4,1-diyl](*E*)ethene-2,1-diyl]}dibenzaldehyde (16). The reaction was performed in a heat-gun-dried 25 mL Schlenk tube under a nitrogen atmosphere. Compounds **11** (200 mg, 71.0 μmol, 1.00 equiv) and **15** (27.4 mg, 156 μmol, 2.20 equiv) were dissolved in dry DMF (5 mL). $Pd(OAc)_2$ (1.59 mg, 7.07 μmol, 0.10 equiv), tris(*o*-tolyl)-phosphine (8.61 mg, 28.3 μmol, 0.40 equiv), and triethylamine (0.5 mL) were added. The mixture was stirred at 125 °C for 48 h. After the reaction mixture was cooled to room temperature, it was poured into 50 mL of water to give a yellow suspension that was extracted with dichloromethane (5 × 50 mL) until the aqueous layer was colorless. The combined organic layers were washed with brine and dried over $MgSO_4$.

Deprotection. The crude product (149 mg, 50.9 μmol, 1.00 equiv) was then dissolved in toluene (5 mL), and a catalytic amount of iodine was added. The mixture was refluxed for 6 h and then quenched with a saturated aqueous solution of $NaSO_3$. The layers were separated, and the aqueous layer was extracted with dichloromethane (4 × 10 mL). The combined organic extracts were dried over $MgSO_4$, and the solvents were evaporated. Column chromatography (silica gel, petroleum ether/dichloromethane/ethyl acetate/methanol = 5:3:1:1.5, R_f = 0.32) afforded **16** as a bright yellow oil (122 mg,

dx.doi.org/10.1021/jo501129d | *J. Org. Chem.* XXXX, XXX, XXX−XXX

43.0 μmol, 84% over 2 steps). IR (cm^{-1}): 2868, 1693, 1595, 1566, 1494, 1455, 1416, 1349, 1304, 1248, 1197, 1095, 959, 849, 819, 516. ^1H NMR (300 MHz, $CDCl_3$): δ 9.99 (s, 2H), 7.87 (d, J = 8.2 Hz, 4H), 7.73−7.68 (m, 6H), 7.41−7.36 (m, 6H), 7.25 (s, 4H), 7.14 (d, J = 16.4 Hz, 2H), 4.59 (quin, J = 5.0 Hz, 2H), 4.51−4.46 (m, 4H), 3.80−3.75 (m, 24H), 3.67−3.56 (m, 120H), 3.51−3.49 (m, 24H), 3.34−3.33 (m, 36H). ^{13}C NMR (150 MHz, $CDCl_3$): δ 191.8, 151.5, 151.0, 150.9, 144.3, 135.2, 130.4, 130.1, 129.4, 128.3, 127.5, 127.1, 124.6, 123.7, 115.3, 114.4, 113.8, 79.8, 79.4, 79.3, 72.0, 71.2−71.1, 70.7−70.6, 59.1. HRMS (MALDI): m/z $[M + H]^+$ calcd for $C_{142}H_{235}O_{56}$ 2836.5541, found 2836.5552.

■ ASSOCIATED CONTENT

Supporting Information

Figures of the ^1H NMR and ^{13}C NMR spectra of all newly synthesized compounds and Cartesian coordinates of the calculated model compounds. This material is available free of charge via the Internet at http://pubs.acs.org.

■ AUTHOR INFORMATION

Corresponding Author

*E-mail: uwe.bunz@oci.uni-heidelberg.de.

Notes

The authors declare no competing financial interest.

■ ACKNOWLEDGMENTS

We thank the SI Fonds of the State of Baden-Württemberg.

■ REFERENCES

(1) (a) Greene, N. T.; Shimizu, K. D. *J. Am. Chem. Soc.* **2005**, *127*, 5695−5700. (b) Merchant, Z. M.; Cheng, S. G. G. In *Characterization of Foods, Emerging Methods*; Gaonkar, A. G., Ed.; Elsevier Science: New York, 1995; Chapter 15. (c) Zhou, H. C.; Baldini, L.; Hong, J.; Wilson, A. J.; Hamilton, A. D. *J. Am. Chem. Soc.* **2006**, *128*, 2421−2425. (d) Yeh, C. Y.; Lin, S. J.; Hwang, D. F. *J. Food Drug Anal.* **2004**, *12*, 128−132.

(2) (a) Mohr, G. J.; Demuth, C.; Spichiger-Keller, U. E. *Anal. Chem.* **1998**, *70*, 3868−3873. (b) Mohr, G. J. *Chem.—Eur. J.* **2004**, *10*, 1082−1090.

(3) (a) Brown, A. S.; Bernal, L. M.; Micotto, T. L.; Smith, E. L.; Wilson, J. N. *Org. Biomol. Chem.* **2011**, *9*, 2142−2148. (b) Dhuguru, J.; Gheewala, C.; Kumar, N. S. S.; Wilson, J. N. *Org. Lett.* **2011**, *13*, 4188−4191.

(4) (a) Zucchero, A. J.; McGrier, P. L.; Bunz, U. H. F. *Acc. Chem. Res.* **2010**, *43*, 397−408. (b) McGrier, P. L.; Solntsev, K. M.; Miao, S.; Tolbert, L. M.; Miranda, O. R.; Rotello, V. M.; Bunz, U. H. F. *Chem.—Eur. J.* **2008**, *14*, 4503−4510.

(5) (a) Nelson, T. L.; O'Sullivan, C.; Greene, N. T.; Maynor, M. S.; Lavigne, J. J. *J. Am. Chem. Soc.* **2006**, *128*, 5640−5641. (b) Maynor, M. S.; Nelson, T. L.; O'Sullivan, C.; Lavigne, J. J. *Org. Lett.* **2007**, *9*, 3217−3220. (c) Nelson, T. L.; Tran, I.; Ingallinera, T. G.; Maynor, M. S.; Lavigne, J. J. *Analyst* **2007**, *132*, 1024−1030.

(6) Rakow, N. A.; Sen, A.; Janzen, M. C.; Ponder, J. B.; Suslick, K. S. *Angew. Chem., Int. Ed.* **2005**, *44*, 4528−4532.

(7) (a) Mertz, E.; Zimmerman, S. E. *J. Am. Chem. Soc.* **2003**, *125*, 3424−3425. (b) Mertz, E.; Beil, J. B.; Zimmerman, S. C. *Org. Lett.* **2003**, *5*, 3127−3130. (c) Feuster, E. K.; Glass, T. E. *J. Am. Chem. Soc.* **2003**, *125*, 16174−16175. (d) Plante, J. P.; Glass, T. E. *Org. Lett.* **2006**, *8*, 2163−2166. (e) Secor, K. E.; Glass, T. E. *Org. Lett.* **2004**, *6*, 3727−3730.

(8) Ellison, C. J.; Miller, K. E.; Torkelson, J. M. *Polymer* **2004**, *45*, 2623−2632.

(9) (a) Patze, C.; Brödner, K.; Rominger, F.; Trapp, O.; Bunz, U. H. F. *Chem.—Eur. J.* **2011**, *17*, 13720−13725. (b) Kumpf, J.; Bunz, U. H. F. *Chem.—Eur. J.* **2012**, *18*, 8921−8924. (c) Freudenberg, J.; Kumpf, J.; Schäfer, V.; Sauter, E.; Wörner, S. J.; Brödner, K.; Dreuw, A.; Bunz, U. H. F. *J. Org. Chem.* **2013**, *78*, 4949−4959. (d) Kumpf, J.; Freudenberg, J.; Schwaebel, S. T.; Bunz, U. H. F. *Macromolecules* **2014**, *47*, 2569−2573.

(10) (a) Mastalerz, M.; Schneider, W.; Oppel, I. M.; Presly, O. *Angew. Chem., Int. Ed.* **2011**, *50*, 1046−1051. (b) Schneider, M. W.; Oppel, I. M.; Mastalerz, M. *Chem.—Eur. J.* **2012**, *18*, 4156−4160. (c) Mastalerz, M.; Hauswald, H.-J. S.; Stoll, R. *Chem. Commun.* **2012**, *48*, 130−132.

(11) (a) Phillips, R. L.; Kim, I. B.; Tolbert, L. M.; Bunz, U. H. F. *J. Am. Chem. Soc.* **2008**, *130*, 6952−6954. (b) Phillips, R. L.; Miranda, O. R.; You, C. C.; Rotello, V. M.; Bunz, U. H. F. *Angew. Chem.* **2008**, *47*, 2590−2594. (c) Khan, A.; Müller, S.; Hecht, S. *Chem. Commun.* **2005**, 584−586.

(12) Shopsowitz, K.; Lelj, F.; MacLachlan, M. J. *J. Org. Chem.* **2011**, *76*, 1285−1294.

(13) (a) Casida, M. E. In *Recent Advances in Density Functional Theory*; Chong, D. P., Ed.; World Scientific: Singapore, 1995; Part I, pp 145−192. (b) Dreuw, A.; Head-Gordon, M. *Chem. Rev.* **2005**, *105*, 4009−4037.

(14) Neese, F. *WIREs Comput. Mol. Sci.* **2012**, *2*, 73−78.

(15) Harbach, P. H. P.; Dreuw, A. In *The Art of Choosing the Right Quantum in Modeling of Molecular Properties*; Comba, P., Ed.; Wiley-VCH: Weinheim, 2011; pp 29−47.

(16) Schwaebel, T.; Menning, S.; Bunz, U. H. F. *Chem. Sci.* **2014**, *5*, 1422−1428.

(17) (a) Schwaebel, T.; Trapp, O.; Bunz, U. H. F. *Chem. Sci.* **2013**, *4*, 273−281. (b) Davey, E. A.; Zucchero, A. J.; Trapp, O.; Bunz, U. H. F. *J. Am. Chem. Soc.* **2011**, *133*, 7716−7718.

(18) Hathaway, B. A.; White, K. L.; McGill, M. E. *Synth. Commun.* **2007**, *37*, 3855−3860.

(19) Sontag, B.; Rüth, M.; Spiteller, P.; Arnold, N.; Steglich, W.; Reichert, M.; Bringmann, G. *Eur. J. Org. Chem.* **2006**, 1023−1033.

(20) Wessendorf, F.; Grimm, B.; Guldi, D. M.; Hirsch, A. *J. Am. Chem. Soc.* **2010**, *132*, 10786−10795.

(21) Fulmer, G. R.; Miller, A. J. M.; Sherden, N. H.; Gottlieb, H. E.; Nudelman, A.; Stoltz, B. M.; Bercaw, J. E.; Goldberg, K. I. *Organometallics* **2010**, *29*, 2176−2179.

(22) Würth, C.; Grabolle, M.; Pauli, J.; Spieles, M.; Resch-Genger, U. *Nat. Protoc.* **2013**, *8*, 1535−1550.